Localized Ferromagnetic Resonance in Inhomogeneous Thin Films

R. D. McMichael and D. J. Twisselmann
National Institute of Standards & Technology, Gaithersburg, Maryland 20899, USA

Andrew Kunz
Physics Department, Lawrence University, Appleton Wisconsin 54912, USA
(Received 23 December 2002; published 3 June 2003)

The effect of sample inhomogeneity on the ferromagnetic resonance linewidth is determined by diagonalization of a spin wave Hamiltonian for ferromagnetic thin films with inhomogeneities spanning a wide range of characteristic length scales. A model inhomogeneity is used that consists of size D grains and an anisotropy field H_p that varies randomly from grain to grain in a film with thickness d and magnetization M_s. The resulting linewidth agrees well with the two-magnon model for small inhomogeneity, $H_pD \ll \pi M_s d$. For large inhomogeneity, $H_pD \gg \pi M_s d$, the precession becomes localized and the spectrum approaches that of local precession on independent grains.

DOI: 10.1103/PhysRevLett.90.227601 PACS numbers: 76.50.+g, 75.40.Gb, 75.40.Mg

In many ferromagnetic materials, a few nanoseconds are typically required for magnetization precession to damp out after the magnetization is rotated away from the equilibrium direction. As data rates approach 1 GHz, this nanosecond time scale for damping becomes a critical issue for data storage and other magnetic applications. Accordingly, there has recently been a surge of interest in magnetization damping, i.e., the coupling of the magnetization to the thermal bath [1–8], and the related magnetic fluctuations in submicron magnetic sensors [9,10].

Ferromagnetic resonance (FMR) is the most prominently used technique to measure magnetization damping. FMR spectra are typically measured either by measuring a pulse response in the time domain [11] or, more commonly, by driving the magnetization with a constant frequency microwave field while slowly changing the resonance frequency via an applied magnetic field H. Damping is measured through the linewidth ΔH of the absorption peak in the transverse susceptibility spectrum.

A central difficulty in the measurement of magnetization damping by ferromagnetic resonance is that experimental values of damping time or FMR linewidth reflect the effects of both inhomogeneity and damping. This Letter describes modeling of FMR line broadening in inhomogeneous thin films through calculations of the eigenmodes of the magnetization motion. The model described below unifies the local resonance model, which is valid for large, strong inhomogeneities, and the two-magnon model, which is valid for small, weak inhomogeneities.

The resonant precession frequency of the magnetization depends on a number of experimental and materials parameters, x_i, including applied field, magnetization, surface anisotropy, film thickness, and magnetocrystalline anisotropy. The simplest model of FMR linewidth and inhomogeneity attributes the inhomogeneous broadening to parameter variations Δx_i that produce different resonance conditions in independent parts of the film [12]. The resulting spread of resonance frequencies yields a field linewidth that is given by

$$\Delta H^{\rm local} = \left(\frac{\partial \omega}{\partial H}\right)^{-1} \sum_i \left|\frac{\partial \omega}{\partial x_i}\right| \Delta x_i + \frac{2}{\sqrt{3}} \alpha \frac{\omega}{\gamma}, \qquad (1)$$

where the last term represents the linewidth due to damping and α is the phenomenological Gilbert damping parameter. In the following, this model will be referred to as the "local resonance" model of linewidth. This model has provided a good description of FMR linewidth data as a function of magnetization angle in several cases [12–14]. Additionally, if the important inhomogeneous effective fields H_p corresponding to parameters x_i simply add to the applied field, the first term in (1) is a constant, and the linewidth is linear in frequency:

$$\Delta H^{\rm local} = H_p + \frac{2}{\sqrt{3}} \alpha \frac{\omega}{\gamma}. \qquad (2)$$

The frequency dependence of ΔH in ultra-thin magnetic metal films is often found to be approximately linear in this way [13,15–17].

The essential assumption of the local resonance model of linewidth is that neighboring regions of the film do not interact significantly. However, exchange and dipolar interactions are essential characteristics of ferromagnetic materials. The two-magnon model of linewidth [18–24], reviewed below, accounts for interactions through the spin wave dispersion relation and treats the inhomogeneity as a perturbation. Two-magnon and local resonance linewidths behave very differently, but the two-magnon model has also been verified by a different set of experimental results [18,25,26].

In the following, we briefly review some of the properties of spin waves, and use them as a basis for modeling linewidth in inhomogeneous films.

Our review of spin waves begins with a uniform magnetic film lying in the x-z plane with an applied field H

along the z direction. For small deviations of the magnetization from its equilibrium, $M_s\hat{\mathbf{z}}$, we write

$$\mathbf{M}(\mathbf{r}) \simeq m_x(\mathbf{r})\hat{\mathbf{x}} + m_y(\mathbf{r})\hat{\mathbf{y}} + M_s\hat{\mathbf{z}}. \quad (3)$$

It is convenient to expand the magnetization in terms of the Fourier coefficients of the magnetization; $m_x(\mathbf{r}) = \sum_{\mathbf{k}} m_{x,\mathbf{k}} e^{i\mathbf{k}\cdot\mathbf{r}}$, and similarly for $m_y(\mathbf{r})$. Neglecting a constant term, the energy of the uniform film can be expanded as

$$E_0 = \frac{V\mu_0}{2}\sum_{\mathbf{k}}(h_{x,\mathbf{k}} m_{x,\mathbf{k}}^2 + h_{y,\mathbf{k}} m_{y,\mathbf{k}}^2), \quad (4)$$

where V is the volume of the film. We assume that the magnetization is uniform across the thickness of the film; the wave vector $\mathbf{k}$ is therefore restricted to the x-z plane. The normalized stiffness fields, $h_{x,\mathbf{k}}$ and $h_{y,\mathbf{k}}$, include the applied field, dipolar fields, and exchange interactions. For a film of thickness d with exchange stiffness A [18,27],

$$M_s h_{x,\mathbf{k}} = H + (2A/M_s)k^2 + (1 - N_k)M_s k_x^2/k^2, \quad (5)$$

$$M_s h_{y,\mathbf{k}} = H + (2A/M_s)k^2 + N_k M_s, \quad (6)$$

where $N_k = (1 - e^{-kd})/kd$ is a k-dependent demagnetization factor [28] under the assumption that the magnetization is uniform through the film thickness. The spin wave dispersion relation is given by

$$\omega_{\mathbf{k}} = \gamma M_s \mu_0 (h_{x,\mathbf{k}} h_{y,\mathbf{k}})^{1/2}, \quad (7)$$

where γ is the gyromagnetic ratio, $g\mu_B/\hbar$; see Fig. 1. In an FMR measurement on an ideal uniform film, the $\mathbf{k} = 0$ uniform mode is resonantly driven by a uniform microwave field and the width of the resonance depends only on damping.

The quantum mechanical raising and lowering operators $a_{\mathbf{k}}^\dagger$ and $a_{\mathbf{k}}$ corresponding to the classical spin waves are given by

$$m_{x_{\mathbf{k}}} = -i\sqrt{\hbar\omega_{\mathbf{k}}/2\mu_0 V h_{x,\mathbf{k}}}(a_{\mathbf{k}} - a_{-\mathbf{k}}^\dagger), \quad (8)$$

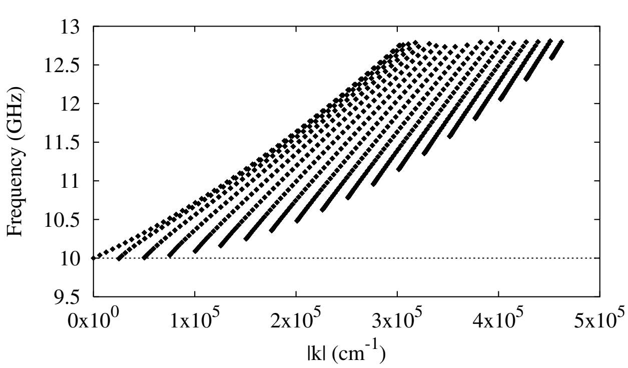

FIG. 1. Precession frequencies of 3001 spin waves for a 3 nm thick rectangle of uniform Permalloy, 10 μm $\times$ 2.5 μm. A 114 mT field is applied in plane to give a uniform precession frequency of $\omega(k = 0)/(2\pi) = 10$ GHz.

$$m_{y_{\mathbf{k}}} = \sqrt{\hbar\omega_{\mathbf{k}}/2\mu_0 V h_{y,\mathbf{k}}}(a_{\mathbf{k}} + a_{-\mathbf{k}}^\dagger). \quad (9)$$

For a simple model of inhomogeneity, we add a spatially varying anisotropy field [18,19]. The energy expression (4) becomes

$$E_p = E_0 + \frac{\mu_0 V_c}{2M_s}\sum_{\mathbf{r}} H_p(\mathbf{r})[m_x(\mathbf{r})^2 + m_y(\mathbf{r})^2], \quad (10)$$

where the sum is over cells of a superimposed 2D grid and V_c is the volume of a grid cell.

The $\mathbf{r}$-dependent terms in (10) are expanded in terms of Fourier coefficients, $H_{p,\mathbf{k}}$, $m_{x,\mathbf{k}}$, and $m_{y,\mathbf{k}}$, which are expanded using Eqs. (8) and (9) to obtain a spin wave Hamiltonian for the inhomogeneous film [29],

$$\mathcal{H} = \hbar\sum_{\mathbf{k}} \omega_{\mathbf{k}} a_{\mathbf{k}}^\dagger a_{\mathbf{k}} + \sum_{\mathbf{k},\mathbf{k}'}[A_{\mathbf{k},\mathbf{k}'} a_{\mathbf{k}'}^\dagger a_{\mathbf{k}} + \text{H.c.}], \quad (11)$$

where H.c. indicates the Hermitian conjugate. Inhomogeneities such as surface pits or voids [20–22] or irregular dipolar and exchange interactions [23] yield Hamiltonians of the same form. For the case of a varying applied field,

$$A_{\mathbf{k},\mathbf{k}'} = \mu_0\gamma\hbar M_s \frac{\sqrt{h_{x,\mathbf{k}} h_{x,\mathbf{k}'}} + \sqrt{h_{y,\mathbf{k}} h_{y,\mathbf{k}'}}}{2\sqrt{\omega_{\mathbf{k}}\omega_{\mathbf{k}'}}} \mu_0\gamma H_{p,\mathbf{k}-\mathbf{k}'}. \quad (12)$$

Terms of the form $A_{0,\mathbf{k}} a_0 a_{\mathbf{k}}^\dagger$ are particularly important for FMR linewidth because they describe the coupling of the uniform mode to spin wave modes.

Treating the A terms in (11) as a perturbation yields the well-known "two-magnon" model for the apparent decay rate $\Gamma^{2\text{mag}}$ of the $\mathbf{k} = 0$ magnon [18–24]. To lowest order in H_p,

$$\Gamma^{2\text{mag}} = \frac{2\pi}{\hbar}\sum_{\mathbf{k}}|A_{0,\mathbf{k}}|^2\delta(\hbar\omega_{\mathbf{k}} - \hbar\omega_0). \quad (13)$$

Peak-to-peak linewidth is taken from the extrema of the derivative spectrum. The corresponding two-magnon contribution to the peak-to-peak, field-swept linewidth is

$$\Delta H^{2\text{mag}} = \frac{1}{\sqrt{3}}\frac{dH}{d\omega_0}\Gamma^{2\text{mag}}. \quad (14)$$

Exchange and dipolar interactions are included in $\Gamma^{2\text{mag}}$ through the spin wave dispersion relation, $\omega_{\mathbf{k}}$, but the validity of (13) is limited to weak perturbations. Higher order extensions of the two-magnon model are needed [30–32].

Here, we move toward finding the linewidth to all orders in H_p by diagonalizing the Hamiltonian (11) numerically [33]. A similar approach was taken by Huber and Ching in a study of density of states and localization in spin clusters with random axis anisotropy [34]. Out of 10^6 eigenmodes of the discretized uniform film, we choose as basis states the 3001 spin waves that are closest in frequency to ω_0, plotted in Fig. 1. For large enough sets of basis states, we find that the calculated linewidth is not sensitive to the number of selected modes. We model $H_p(\mathbf{r})$ by assigning a random field to each grain in a periodic "grain structure" made up of Voronoi polygons. The random field is taken from a Gaussian distribution with root mean square value $H_p^{\rm rms}$.

The diagonalization routine yields the eigenfrequencies of the inhomogeneous film and its eigenmodes b_i. These new eigenmodes are mixtures of the basis spin waves $a_{\mathbf{k}}$; $b_i = \sum_{\mathbf{k}} \mathsf{U}_{i,\mathbf{k}} a_{\mathbf{k}}$ where $\mathsf{U}_{i,\mathbf{k}}$ is the unitary matrix that diagonalizes (11). Because the $\mathbf{k} = 0$ spin wave is generally a component of each eigenmode, each of the eigenmodes can couple directly to the applied uniform microwave field. The FMR intensity I_i of each eigenmode is given by $I_i = |\mathsf{U}_{i,0}|^2$.

We illustrate this procedure by modeling the FMR response of 3 nm-thick films with $M_s = 800$ kA/m ($4\pi M_s = 10$ kG) in an applied field of $\mu_0 H = 114$ mT to give a resonant frequency of 10 GHz. Results are shown for average grain sizes of 20 and 1400 nm in Figs. 2 and 3, respectively.

The FMR intensity distribution is plotted as impulses in Figs. 2(a) and 3(a). For uniform films, these distributions would appear as single spikes at 10 GHz. We simulate FMR signals by replacing each eigenmode spike with a Lorentzian peak, each peak having integrated intensity I_i and having full width at half maximum given by the Landau-Lifshitz-Gilbert linewidth $\Delta\omega_{50} = \alpha\gamma\mu_0 M_s(h_{x,0} + h_{y,0})$ and $\alpha = 0.01$. The individual Lorentzian peaks are summed and the result is differentiated with respect to frequency to obtain the simulated FMR signal. The peak-to-peak frequency linewidth $\Delta\omega$ is determined from the maximum and minimum of this signal, similar to the common experimental practice. Finally, the field linewidth is obtained using $\Delta H = \Delta\omega[dH/d\omega_0]$.

The grain structures and perturbation fields used in these examples are shown in Figs. 2(b) and 3(b) where $H_p(\mathbf{r})$ is lowest in dark grains and highest in light grains. The magnetization patterns associated with single eigenmodes are shown in Figs. 2(c) and 3(c) with grey scale indicating $m_x(\mathbf{r})$. These patterns are calculated using $m_{x,i}(\mathbf{r}) \propto \sum_{\mathbf{k}}(\mathsf{U}_{i,\mathbf{k}} - \mathsf{U}^*_{i,-k})e^{i\mathbf{k}\cdot\mathbf{r}}$. Using this color scheme, uniform precession would appear as a solid light or dark color.

There are a number of qualitative differences between the results for large and small grains. For small grains (Fig. 2) the magnetization precession is on length scales much larger than the grain size and the FMR signal looks Lorentzian. For large grains, (Fig. 3), the magnetization pattern is closely correlated with the grain structure and the spectra are more complicated. These spectra are similar to the results of local resonance calculations where the precession frequency for each grain is calculated from the local applied field $H + H_p(\mathbf{r})$ and the intensity is proportional to the grain area. The FMR signals calculated from the 3001 eigenmodes and from the 51 grains are very similar. [Fig. 3(a)]. For the complicated, large-grain spectra, the peak-to-peak characterization of linewidth does not give consistent results for different grain structures with the same average grain size. As an alternative linewidth characterization for large grains, we calculate the standard deviation of the eigenmode intensity distribution, and report a peak-to-peak linewidth corresponding to a Gaussian peak with the same standard deviation. This method fails for Lorentzian intensity distributions because the standard deviation is not well defined.

In Fig. 4, linewidth values from eigenmode calculations, the two-magnon model, and the local resonance model are plotted as a function of grain size for three values of rms perturbation field. There is a transition from

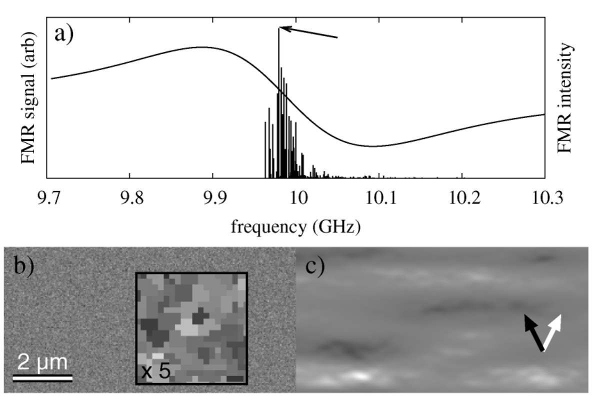

FIG. 2. Calculated FMR response for a 3 nm thick film of Permalloy with 20 nm grains and a 10 mT rms perturbation field. (a) FMR intensity and simulated FMR signal, (b) half of the grain structure, and (c) the corresponding half of the eigenmode indicated by the arrow in (a) showing the collective response of this mode to a uniform driving field.

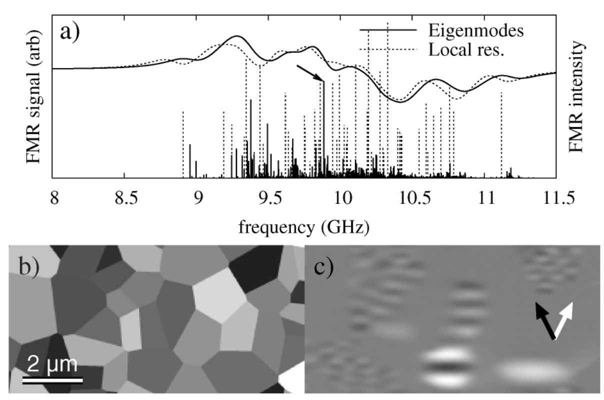

FIG. 3. Calculated FMR response for a 3 nm thick film of Permalloy with 1.4 μm grains and a 10 mT rms perturbation field. (a) FMR intensities and signals calculated from eigenmode intensity and from the local resonance approximation, (b) half of the grain structure, and (c) the corresponding half of the eigenmode indicated by the arrow in (a) showing local precession appearing predominantly in two of the grains.

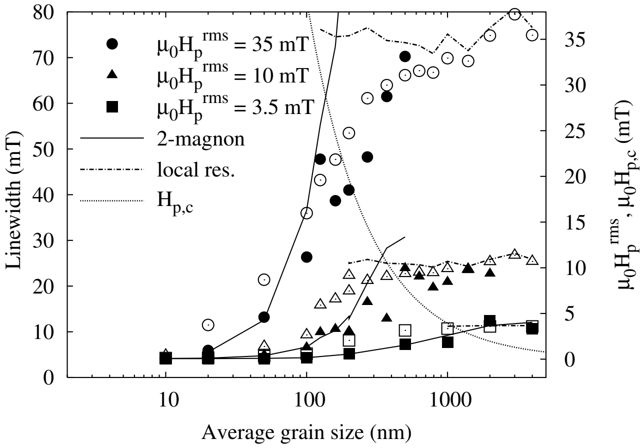

FIG. 4. Peak-to-peak (filled symbols) and standard deviation (open symbols) linewidths as a function of grain size. Results are shown for three values of rms perturbation field, $H_p^{\rm rms}$. The characteristic value of $H_{p,c}$ for the transition from collective to local behavior is shown. The left and right axes are related by Eq. (2).

two-magnon behavior to local resonance behavior that depends on grain size and perturbation field.

The characteristic combination of perturbation field and grain size for the transition from two-magnon behavior to local resonance behavior can be estimated by considering a low-**k** spin wave in a grain of width D where the applied field differs by $H_{p,c}$. If the spin wave with frequency ω is launched in the center of the grain we argue that it will behave locally if it is more than approximately π out of phase at the grain boundaries;

$$\frac{\partial k_y}{\partial H}\bigg|_{\omega} H_{p,c}D = \frac{2(2H+M)}{M_s^2 d} H_{p,c}D \approx 2\pi. \qquad (15)$$

This estimate of $H_{p,c}$ is plotted in Fig. 4. In contrast to this estimate, the Ioffe-Regel criterion for localization [35] suggests that there should never be localization in this system because the mean free path for a magnon is always less than the essentially infinite wavelength of interest.

The eigenmode analysis presented here unifies the two-magnon model and the local resonance model and suggests that the two-magnon model describes not true damping, but only the width of the FMR intensity distribution that remains after inhomogeneities are effectively smoothed by dipolar and exchange interactions.

[1] V. L. Safonov, J. Appl. Phys. **91**, 8653 (2002).
[2] V. L. Safonov and H. N. Bertram, cond-mat/0207721 [J. Appl. Phys. (to be published)].
[3] N. Smith, J. Appl. Phys. **92**, 3877 (2002).
[4] V. Kamberský, Can. J. Phys. **48**, 2906 (1970).
[5] V. Korenman and R. E. Prange, Phys. Rev. B **6**, 2769 (1972).
[6] L. Berger, J. Phys. Chem. Solids **38**, 1321 (1977).
[7] V. L. Safonov and H. N. Bertram, Phys. Rev. B **61**, 14 893 (2000).
[8] S. E. Russek, P. Kabos, R. D. McMichael, C. G. Lee, W. E. Bailey, R. Ewasko, and S. C. Sanders, J. Appl. Phys. **91**, 8659 (2002).
[9] N. Smith and P. Arnett, Appl. Phys. Lett. **78**, 1448 (2001).
[10] H. N. Bertram, V. L. Safonov, and Z. Jin, IEEE Trans. Magn. **38**, 2514 (2002).
[11] T. J. Silva, C. S. Lee, T. M. Crawford, and C. T. Rogers, J. Appl. Phys. **85**, 7849 (1999).
[12] C. Chappert, K. L. Dang, P. Beauvillain, H. Hurdequint, and D. Renard, Phys. Rev. B **34**, 3192 (1986).
[13] W. Platow, A. N. Anisimov, G. L. Dunifer, M. Farle, and K. Baberschke, Phys. Rev. B **58**, 5611 (1998).
[14] S. Mizukami, Y. Ando, and T. Miyazaki, Jpn. J. Appl. Phys. **40**, 580 (2001).
[15] Z. Celinski and B. Heinrich, J. Appl. Phys. **70**, 5935 (1991).
[16] R. Karim, S. D. Ball, J. R. Truesdon, and C. E. Patton, J. Appl. Phys. **73**, 4512 (1993).
[17] D. J. Twisselmann and R. D. McMichael, J. Appl. Phys. **93**, 6903 (2003).
[18] R. D. McMichael, M. D. Stiles, P. J. Chen, and W. F. Egelhoff, Jr., J. Appl. Phys. **83**, 7037 (1998).
[19] C.W. Haas and H. B. Callen, in *Magnetism* (Academic Press, New York, 1963), Vol. 1, Chap. 10, pp. 480–497.
[20] M. Sparks, R. Loudon, and C. Kittel, Phys. Rev. **122**, 791 (1961).
[21] M. Sparks, *Ferromagnetic Relaxation Theory*, Advanced Physics Monograph Series (McGraw-Hill, New York, 1964).
[22] M. J. Hurben and C. E. Patton, J. Appl. Phys. **83**, 4344 (1998).
[23] A. M. Clogston, H. Suhl, L. R. Walker, and P.W. Anderson, J. Phys. Chem. Solids **1**, 129 (1956).
[24] R. Arias and D. L. Mills, Phys. Rev. B **60**, 7395 (1999).
[25] R. D. McMichael, D. J. Twisselmann, J. E. Bonevich, A. P. Chen, W. F. Egelhoff, and S. E. Russek, J. Appl. Phys. **91**, 8647 (2002).
[26] C. E. Patton, Phys. Rev. **179**, 352 (1969).
[27] B. A. Kalinikos and A. N. Slavin, J. Phys. C **19**, 7013 (1986).
[28] K. J. Harte, J. Appl. Phys. **39**, 1503 (1968).
[29] Terms including $a_{\mathbf{k}}^\dagger a_{\mathbf{k}'}^\dagger$ and $a_{\mathbf{k}} a_{\mathbf{k}'}$, which mostly affect the ellipticity of the precession, have been dropped.
[30] E. Schlömann, Phys. Rev. **182**, 632 (1969).
[31] Q. H. F. Vrehen, J. Appl. Phys. **40**, 1849 (1969).
[32] Q. H. F. Vrehen, A. B. van Groenou, and J. G. M. de Lau, Solid State Commun.. **7**, 117 (1969).
[33] A. Kunz and R. D. McMichael, IEEE Trans. Magn. **38**, 2400 (2002).
[34] D. L. Huber and W.Y. Ching, Phys. Rev. B **39**, 4453 (1989).
[35] A. F. Ioffe and A. R. Regel, in *Progress in Semiconductors*, edited by A. F. Gibson (Wiley, New York, 1960), Vol. 4, p. 237.